Photothermal Effects Hot Paper

International Edition: DOI: 10.1002/anie.201505534
German Edition: DOI: 10.1002/ange.201505534

Thermosensitive Ion Channel Activation in Single Neuronal Cells by Using Surface-Engineered Plasmonic Nanoparticles

*Hirotaka Nakatsuji, Tomohiro Numata, Nobuhiro Morone, Shuji Kaneko, Yasuo Mori, Hiroshi Imahori, and Tatsuya Murakami**

Abstract: *Controlling cell functions using external photoresponsive nanomaterials has enormous potential for the development of cell-engineering technologies and intractable disease therapies, but the former currently requires genetic modification of the target cells. We present a method using plasma-membrane-targeted gold nanorods (pm-AuNRs) prepared with a cationic protein/lipid complex to activate a thermosensitive cation channel, TRPV1, in intact neuronal cells. Highly localized photothermal heat generation mediated by the pm-AuNRs induced Ca^{2+} influx solely by TRPV1 activation. In contrast, the use of previously reported cationic AuNRs that are coated with a conventional synthetic polymer also led to photoinduced Ca^{2+} influx, but this influx resulted from membrane damage. Our method provides an optogenetic platform without the need for prior genetic engineering of the target cells and might be useful for novel TRPV1-targeted phototherapeutic approaches.*

The photocontrol of endogenous neuronal cells could provide an appealing optogenetic method; for example, such localized stimulation by near-infrared (NIR) illumination might potentially be utilized as a non-invasive therapeutic modality.[1] However, current optogenetic approaches generally require prior genetic modification of the target cells,[2] which limits their broad application. The transient receptor potential vanilloid type 1 (TRPV1) is a Ca^{2+} permeable polymodal channel gated by noxious physical and chemical stimuli, including heat ($>43\,^{\circ}C$), low pH values (<5.2), capsaicin, and the *Euphorbia* toxin resiniferatoxin.[3] TRPV1 is present in both the peripheral and central nervous systems; in the latter, its expression is restricted to small- and medium-sized dorsal root ganglion (DRG) neurons. TRPV1 might serve as a therapeutic target in DRG neurons[4] and in other cells;[5] however, localized stimulation of TRPV1 in neurons by external stimuli has not yet been demonstrated. Herein, we sought to develop a method for the safe photothermal heating of TRPV1 on the surface of a single intact neuron by NIR light.

Localized heating with plasmonic nanoparticles is an emerging technology for lipid bilayers. The photoinduced generation of transient nanopores has been shown to allow the flow of biological substances into live cells[6] and artificial lipid bilayers.[7] These results motivated us to propose a more sophisticated plasma membrane (PM) heating system relevant to optogenetics as well as to phototherapy, namely the photoactivation of TRPV1 with gold nanorods (AuNRs), which are plasmonic nanoparticles that absorb minimally invasive NIR light to generate heat,[8] because we could previously show that AuNRs coated with a genetically cationized form of high-density lipoprotein (HDL) were able to bind to cells with very high efficiency and without cytotoxicity.[9] This procedure was shown to be applicable not only to AuNRs but also to other metal nanoparticles with different shapes and compositions. Like HDL, mutated HDL also has a discoidal structure indicating the existence of a neutral phospholipid bilayer circumscribed with cationic peptide-fused lipid-binding protein(s). We concluded that upon binding of the mutated HDLs to AuNRs, their discoidal membranes fused with each other to yield a smooth organic layer with a thickness comparable to that of phospholipid bilayers.

The utilization of electrostatic interactions would be the simplest strategy to target AuNRs to the PM. As-synthesized AuNRs stabilized with the cationic dispersant cetyltrimethylammonium bromide interact well with cells. However, the enhanced cell interaction of such cationic nanoparticles is often accompanied by compromised membrane integrity,[10] which could lead to permeabilization and associated cytotoxicity, which are counterproductive for effective membrane channel photocontrol. Therefore, the choice of an appropriate dispersant to stabilize and cationize the AuNRs is crucial. In this study, we employed a further cationized form of HDL (catHDL, see the Supporting Information) as a dispersant and compared its effects with those of the well-known cationic synthetic polymers poly(diallyldimethylammonium chloride) (PDDAC), polyethyleneimine (PEI), and poly(L-lysine) (PLL).

AuNRs with a plasmonic absorption maximum at 785 nm were coated with catHDL according to our previous report or

[*] Dr. N. Morone, Prof. H. Imahori, Dr. T. Murakami
Institute for Integrated Cell-Material Sciences (WPI-iCeMS)
Kyoto University
Sakyo-ku, Kyoto 606-8501 (Japan)
E-mail: murakami@icems.kyoto-u.ac.jp
H. Nakatsuji, Prof. H. Imahori
Department of Molecular Engineering
Graduate School of Engineering, Kyoto University
Nishikyo-ku, Kyoto 615-8510 (Japan)
Dr. T. Numata, Prof. Y. Mori
Department of Synthetic Chemistry and Biological Chemistry
Graduate School of Engineering, Kyoto University
Nishikyo-ku, Kyoto 615-8510 (Japan)
Prof. S. Kaneko
Department of Molecular Pharmacology
Graduate School of Pharmaceutical Sciences, Kyoto University
Sakyo-ku, Kyoto 606-8501 (Japan)

Supporting information for this article is available on the WWW under http://dx.doi.org/10.1002/anie.201505534.

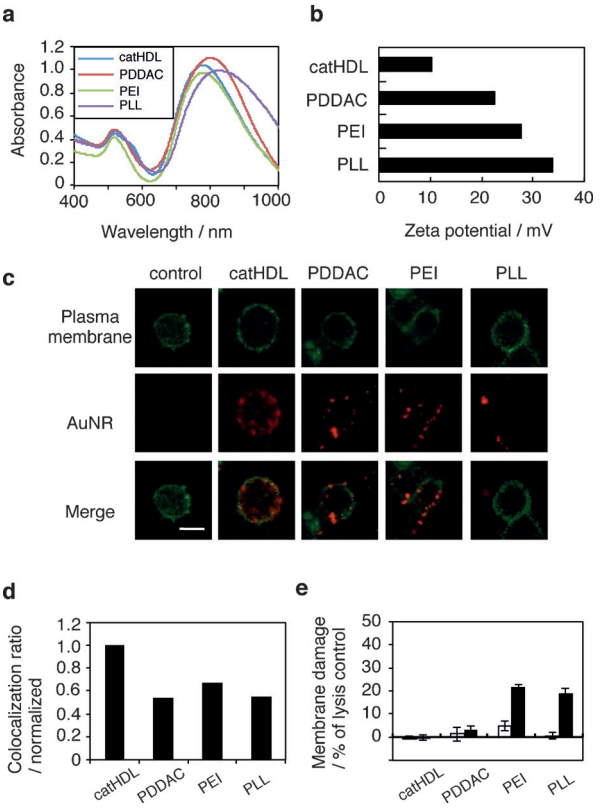

Figure 1. Characterization of surface-functionalized AuNRs. a) Vis/NIR absorption spectra of various AuNRs in PBS. Various peak wavelengths are seen, probably owing to the local dielectric functions of the dispersants and/or different colloidal stabilities.[13] b) Zeta potentials of the AuNRs, which are positive for all AuNRs. c) Two-photon luminescence microscopy images of HEK293T cells treated with various AuNRs ($A_{780}=0.15$, 10 min). The signals derived from the AuNRs and the pEGFP-f staining of the PM are shown in red and green, respectively. Only pm-AuNRs appear to colocalize well with the PM. Scale bar: 10 μm. d) Colocalization ratios of AuNR and EGFP fluorescence. The colocalization ratio is defined as the number of red pixels colocalizing with the green pixels in the cells divided by the total number of red pixels in the cells. Higher ratios indicate greater AuNR binding to the PM. The pm-AuNRs exhibit the most effective binding to the PM among the various NRs tested. e) Lactate dehydrogenase assay data for cells treated with various AuNRs at $A_{780}=0.15$ (white bar) or 0.3 (black bar) for 10 min. Data are normalized to both non-treated (0% membrane damage) and 0.02% Tween 20 treated (100% membrane damage) cells. The pm-AuNRs demonstrated the weakest cytotoxicity among the AuNRs examined.

with PDDAC, PEI, or PLL by a layer-by-layer electrostatic assembly method,[11] which stabilized the AuNRs to different degrees (Figure 1a). The presence of catHDL and the synthetic cationic polymers on the AuNR surface was confirmed by analysis of the Zeta potential and IR spectroscopy (Figure 1b; see also the Supporting Information, Figure S1). PM binding of the cationized AuNRs was examined by observing their two-photon luminescence (TPL; Figure 1c) because the TPL intensity provides an indication of the colloidal stability of the AuNRs on the PM.[12] Only catHDL-treated AuNRs (pm-AuNRs) were found to bind adequately to HEK293T PMs following AuNR treatment for 10 min ($A_{780}=0.15$; Figure 1d). Furthermore, pm-AuNRs had the weakest cytotoxicity (Figure 1e), although the degree of cationization was similar for all samples (Figure 1b). The pm-AuNR phospholipid bilayer might reduce the membrane disruption induced by the cationic polymers, and the protein moiety could enhance the colloidal stability of the pm-AuNRs even on the PM. Accordingly, we decided to further pursue pm-AuNRs.

TRPV1 photoactivation by pm-AuNRs (Figure 2a) was evaluated in a Ca^{2+} flux assay based on fluorescence detection of a Ca^{2+} indicator, Fluo3-AM, using an epifluorescence

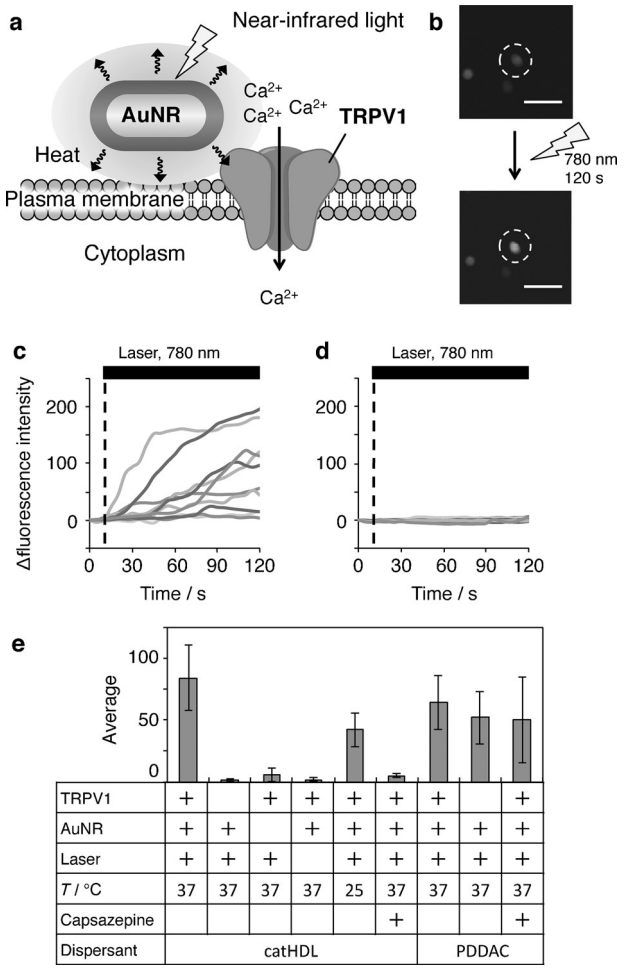

Figure 2. Photoactivation of TRPV1-overexpressing HEK293T cells by AuNRs. a) Schematic representation of the localized photothermal heating of a TRPV1-expressing PM bearing pm-AuNRs. Transduced cells were loaded with an intracellular Ca^{2+} indicator, Fluo 3-AM (Dojindo), treated with pm-AuNRs ($A_{780}=0.15$), and then illuminated at 780 nm (8 $\mu W\,\mu m^{-2}$) under incubation at 37 °C. b) Fluorescence images of cells before and after illumination. Dotted circles indicate the illuminated area. Scale bar: 100 μm. c,d) Time-dependent changes in the fluorescence intensities of transduced (c) and intact cells (d) under illumination. Each curve was obtained from a single cell. e) The average and standard deviation values for the maximal fluorescence intensities during 120 s illumination under various conditions. The TRPV1 dependence of the photoactivation was further examined by adding the TRPV1 antagonist capsazepine. Capsazepine treatment completely inhibits the Ca^{2+} influx induced by pm-AuNRs under illumination. In contrast, AuNRs cationized with PDDAC are not able to induce TRPV1-dependent Ca^{2+} influx.

microscope equipped with a wavelength-tunable laser (715–950 nm; Figure S2). Upon illumination at 780 nm (8 $\mu W\,\mu m^{-2}$) of a single TRPV1-overexpressing HEK293T cell bearing pm-AuNRs on the PM, the fluorescence intensity increased (Figure 2b), and the degree of this increase depended on the illumination time (Figure 2c). This Ca^{2+} influx was not detected in the absence of either TRPV1 expression (Figure 2d), pm-AuNR treatment (Figure S3a), or illumination (Figure S3b), and was suppressed by half at a lower incubation temperature (Figure S3c). These results, which are summarized in Figure 2e, unambiguously corroborate that PM-bound AuNRs photoactivated TRPV1 by photothermal heat generation without membrane disruption.

We next evaluated the potentially adverse effects of this photoactivation. The addition of capsazepine, a TRPV1 antagonist, throughout (Figures S3d and S2e) or halfway through (Figure S3e) photoactivation almost completely blocked Ca^{2+} influx, suggesting that localized heat generation evinced negligible detrimental effects on TRPV1. As shown in Figure S4, no indications of necrosis or apoptosis were detected after photoactivation.

PDDAC-stabilized AuNRs, which showed the lowest cytotoxicity in the dark among the cationic-polymer-coated AuNRs examined (Figure 1e), also yielded a photoinduced Ca^{2+} influx, but this was independent of both TRPV1 expression and function (Figure 2e) and the laser power intensity (Figure S5), suggesting that this effect was due to membrane disruption, potentially because of less uniform heat generation (Figure 1c) and the associated damage, rather than TRPV1 activation.[14] Similarly, it has been reported that the photodynamic and photothermal effects of photosensitizer-loaded carbon nanoparticles could additively induce Ca^{2+} influx in various types of cells including macrophages by unknown mechanisms, but in these cases, the involvement of membrane disruption could not be excluded.[15] In contrast to the results of that work, our results demonstrate that pm-AuNRs enable the safe activation of a defined single type of ion channel solely by localized photothermal heating of the PM, thus highlighting the importance of AuNR surface chemistry.

To confirm that photoactivation was caused by a local temperature rise, the temperature dependences of the fluorescence intensities[16] of 1,2-dioleoyl-*sn*-glycero-3-phosphoethanolamine-*N*-(lissamine rhodamine B sulfonyl) (Rho-PE) incorporated into pm-AuNR and of LysoTracker Green DND-26 localized in late endosomes/lysosomes were used as thermometers (Figures S6 and S7a). Upon laser illumination, on average, the temperature of the PM reached over 43 °C within 120 s, whereas the temperature of the late endosomes/lysosomes remained unchanged (Figure S7b). These data also exemplify that the photothermal heating by pm-AuNRs acts as the trigger for TRPV1 activation and is confined to the immediate PM vicinity.

We also compared the photoactivation efficiencies of the pm-AuNRs at various laser wavelengths around the absorption peak (780 nm) to verify the importance of plasmon resonance absorption. We found that the relative Ca^{2+} influx increased only at 780 nm or shorter wavelengths and was greatly suppressed at the other tested wavelengths (Figure 3a–e). These results seem to contradict the plasmon absorption profile of the pm-AuNRs, which had the same absorbance at 730 and 830 nm and at 715 and 855 nm (80 and 60% of the absorbance at 780 nm, respectively; Figure 1a), because the degree of temperature elevation for AuNR dispersions illuminated at various wavelengths was entirely dependent on the absorbance of the pm-AuNRs (Figure S8). Cell–nanoparticle interactions have been reported to be affected by the size and shape of the nanoparticles,[17] which also greatly influence the plasmon resonance absorption of

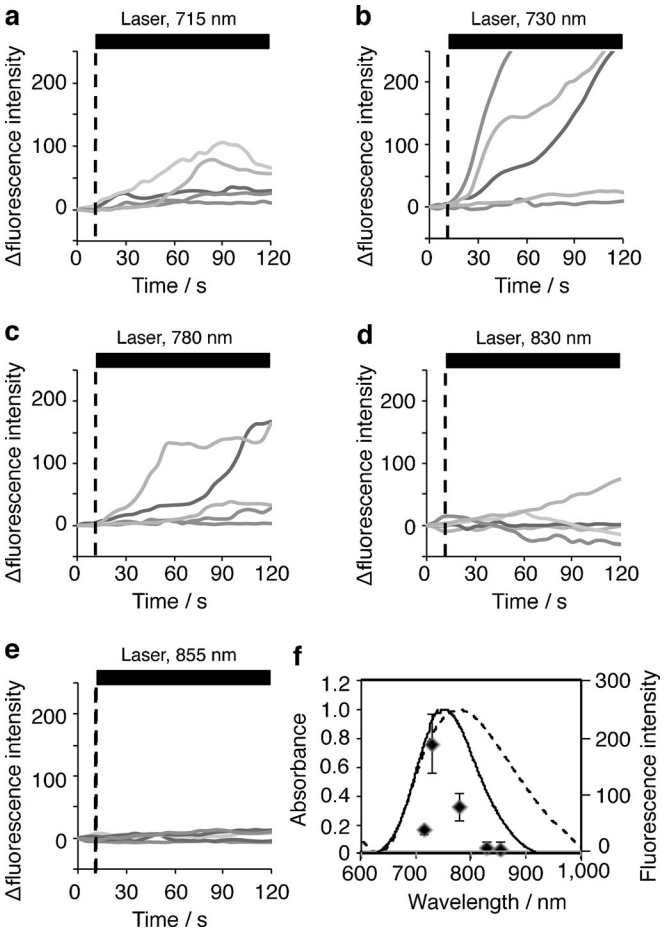

Figure 3. Plasmonic enhancement of TRPV1 photoactivation. TRPV1-overexpressing HEK293T cells bearing pm-AuNRs were illuminated at a) 715, b) 735, c) 780, d) 830, and e) 855 nm. Compared to the absorbance at 780 nm (reflecting the plasmon absorption maximum of the pm-AuNRs), the absorbance values at 715 and 855 nm and at 730 and 830 nm were 60% and 80%, respectively (Figure 1a). f) The Vis/NIR absorption spectra of the pm-AuNRs in HBSS before cell treatment (dashed curve) and of the cell-adsorbed fraction of pm-AuNRs (solid curve). The latter is the differential absorption spectrum obtained by subtracting the spectrum of the cell supernatant containing unbound pm-AuNRs from the spectrum of pm-AuNRs before cell treatment. In (f), the average and standard deviation data for the maximum fluorescence intensities during 120 s illumination for ten cells in (a)–(e) are also shown as a scatter diagram. The plasmon absorption peak of the cell-adsorbed fraction of the pm-AuNRs is blue-shifted from 780 nm to 745 nm, and this plasmon absorption profile is in accordance with the data shown in the scatter diagram. This plasmon resonance blue shift indicates a preferential binding of the lower-aspect-ratio fractions of the pm-AuNRs.[8]

the AuNRs. To determine the cell-adsorbed fraction of the pm-AuNRs, a differential absorption spectrum was obtained by subtracting the spectrum of the cell supernatant from that of the original pm-AuNRs; consequently, the absorption maximum was found to be blue-shifted from 780 to 745 nm (Figure 3 f), and the actual absorption intensities were estimated to decrease with the wavelength in the order 735 > 780 > 715 > 830 > 855 nm, in accordance with the fluorescence intensity data summarized in Figure 3 f. Furthermore, we found that photoinduced TRPV1-dependent Ca^{2+} influx became possible even at 812 nm, with half of the absorbance at 780 nm, when the laser power intensity was doubled (Figure S9). These results emphasize the importance of the plasmon resonance of the AuNRs for TRPV1 photoactivation.

Finally, the feasibility of our method for TRPV1 photoactivation under nearly physiological conditions was assessed in primary cultured DRG neurons from wild type (WT) mice (some of which express TRPV1) as well as from TRPV1 knockout (KO) mice. As shown in Figure 4, pm-AuNRs achieved photoinduced Ca^{2+} influx in primary cultured DRGs

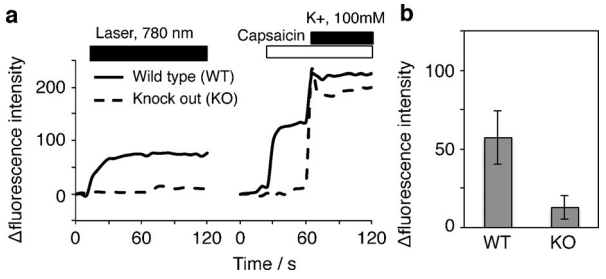

Figure 4. Photoactivation of primary cultured neuronal cells by AuNRs. a) Ca^{2+} influx photoinduced in DRG neurons of WT and TRPV1 KO mice. Representative Ca^{2+} responses in WT (solid line) and KO (broken line) neurons under the same conditions as in Figure 2 are shown. Once the Ca^{2+} concentration in the illuminated WT cells had returned to the basal level, we added capsaicin (1 μM), a TRPV1 agonist, followed by a K^+ solution (100 mM) to induce depolarization to evaluate the TRPV1 expression and neuronal activity of the illuminated cells, respectively. b) Average and standard deviation values of the maximum fluorescence intensities of five cells during 120 s illumination. Five of ten capsaicin-responsive WT cells were photoactivated by the AuNRs.

from WT, but not from TRPV1 KO mice. The neuronal activity of illuminated cells was confirmed by observing the depolarization induced by high K^+ concentrations (Figure 4 a). These results corroborate that our method safely photoactivates TRPV1 under physiological conditions.

Magnetic nanoparticles have also been shown to be able to activate overexpressed TRPV1 channels in HEK293/T cells through localized heating stimulated by the application of a radiofrequency magnetic field.[16a,18] However, although the use of magnetic compounds might allow deep tissue penetration, this strategy required genetic modification of the cells as well as over 1000 times higher nanoparticle concentrations to achieve a similar degree of heating as with plasmonic nanoparticles.[9,18] Therefore, plasmonic nanoparticles currently have a heating power that is at least 1000 times greater than that of magnetic nanoparticles. Furthermore, light provides a more precisely localized stimulation, and the increased rate of photothermal heating compared to that of magnetic-field-induced heating is also advantageous.[19]

Clinically, TRPV1 is a potential therapeutic target for nociceptive pain and cancer.[4,5] The lack of requirement of prior genetic engineering of the target cells for TRPV1 activation under minimally invasive NIR illumination is one of the advantages of our method. Furthermore, compared with small molecules, nanomaterials are retained in the body for a prolonged period of time; therefore, the local injection of pm-AuNRs might enable repetitive and on-demand treatment of these disorders.

In conclusion, we have developed an unprecedented optogenetic means for thermosensitive cation channel activation in the plasma membrane of intact cells using localized photothermal heating of near-infrared plasmonic nanoparticles. The success of this approach was dependent upon modulation of the mesoscopic surface chemistry of the nanoparticles using a cationic lipoprotein, which is an indispensable factor for their uniform and non-cytotoxic PM delivery through suppression of the PM disruption associated with photothermal heating. Furthermore, considering future medical applications, the utilization of material based on human proteins should be beneficial. Our strategy for mesoscopic surface chemistry could also potentially enable the localized photothermal heating of specific intracellular organelles while minimizing thermal membrane damage, opening up novel areas of research.

Acknowledgements

We would like to thank Dr. Hideki Hirori for his assistance and helpful discussions on the laser experiments. We also thank Shouhei Koyama and Tasuku Kimura for their assistance with Ca^{2+} imaging. This work was supported by the World Premier International Research Center Initiative (WPI), the Ministry of Education, Culture, Sports, Science & Technology (MEXT), Japan, and a Grant-in-Aid for Scientific Research (B), MEXT (T.M.).

Keywords: cell engineering · ion channels · nanoparticles · photothermal effects · surface chemistry

How to cite: *Angew. Chem. Int. Ed.* **2015**, *54*, 11725–11729
Angew. Chem. **2015**, *127*, 11891–11895

[1] M. P. Melancon, M. Zhou, C. Li, *Acc. Chem. Res.* **2011**, *44*, 947–956.
[2] a) S. Szobota, E. Y. Isacoff, *Annu. Rev. Biophys.* **2010**, *39*, 329–348; b) D. Tischer, O. D. Weiner, *Nat. Rev. Mol. Cell Biol.* **2014**, *15*, 551–558.
[3] M. Tominaga, M. J. Caterina, A. B. Malmberg, T. A. Rosen, H. Gilbert, K. Skinner, B. E. Raumann, A. I. Basbaum, D. Julius, *Neuron* **1998**, *21*, 531–543.
[4] J. D. Brederson, P. R. Kym, A. Szallasi, *Eur. J. Pharmacol.* **2013**, *716*, 61–76.
[5] a) K. Stock, J. Kumar, M. Synowitz, S. Petrosino, R. Imperatore, E. S. Smith, P. Wend, B. Purfurst, U. A. Nuber, U. Gurok, V. Matyash, J. H. Walzlein, S. R. Chirasani, G. Dittmar, B. F.

Cravatt, S. Momma, G. R. Lewin, A. Ligresti, L. De Petrocellis, L. Cristino, V. Di Marzo, H. Kettenmann, R. Glass, *Nat. Med.* **2012**, *18*, 1232 – 1238; b) P. K. Randhawa, A. S. Jaggi, *Eur. J. Pharmacol.* **2015**, *746*, 180 – 185.
[6] J. Baumgart, L. Humbert, E. Boulais, R. Lachaine, J. J. Lebrun, M. Meunier, *Biomaterials* **2012**, *33*, 2345 – 2350.
[7] L. Paasonen, T. Laaksonen, C. Johans, M. Yliperttula, K. Kontturi, A. Urth, *J. Controlled Release* **2007**, *122*, 86 – 93.
[8] X. Huang, I. H. El-Sayed, W. Qian, M. A. El-Sayed, *J. Am. Chem. Soc.* **2006**, *128*, 2115 – 2120.
[9] T. Murakami, H. Nakatsuji, N. Morone, J. E. Heuser, F. Ishidate, M. Hashida, H. Imahori, *ACS Nano* **2014**, *8*, 7370 – 7376.
[10] J. Lin, H. Zhang, Z. Chen, Y. Zheng, *ACS Nano* **2010**, *4*, 5421 – 5429.
[11] L. Xu, Y. Liu, Z. Chen, W. Li, Y. Liu, L. Wang, Y. Liu, X. C. Wu, Y. Ji, Y. Zhao, L. Ma, Y. Shao, C. Chen, *Nano Lett.* **2012**, *12*, 2003 – 2012.
[12] N. J. Durr, T. Larson, D. K. Smith, B. A. Korgel, K. Sokolov, A. Ben-Yakar, *Nano Lett.* **2007**, *7*, 941 – 945.
[13] a) S. Link, M. B. Mohamed, M. A. El-Sayed, *J. Phys. Chem. B* **1999**, *103*, 3073 – 3077; b) S. Link, M. A. El-Sayed, *J. Phys. Chem. B* **2005**, *109*, 10531 – 10532.
[14] a) A. E. Cress, E. W. Gerner, *Nature* **1980**, *283*, 677 – 679; b) M. A. Mackey, M. R. Ali, L. A. Austin, R. D. Near, M. A. El-Sayed, *J. Phys. Chem. B* **2014**, *118*, 1319 – 1326.
[15] E. Miyako, J. Russier, M. Mauro, C. Cebrian, H. Yawo, C. Menard-Moyon, J. A. Hutchison, M. Yudasaka, S. Iijima, L. De Cola, A. Bianco, *Angew. Chem. Int. Ed.* **2014**, *53*, 13121 – 13125; *Angew. Chem.* **2014**, *126*, 13337 – 13341.
[16] a) H. Huang, S. Delikanli, H. Zeng, D. M. Ferkey, A. Pralle, *Nat. Nanotechnol.* **2010**, *5*, 602 – 606; b) J. Coppeta, C. Rogers, *Exp. Fluids* **1998**, *25*, 1 – 15.
[17] I. Canton, G. Battaglia, *Chem. Soc. Rev.* **2012**, *41*, 2718 – 2739.
[18] S. A. Stanley, J. E. Gagner, S. Damanpour, M. Yoshida, J. S. Dordick, J. M. Friedman, *Science* **2012**, *336*, 604 – 608.
[19] R. Singh, S. V. Torti, *Adv. Drug Delivery Rev.* **2013**, *65*, 2045 – 2060.

Received: June 16, 2015
Published online: August 6, 2015

